
A stellar and nebular model for IC418

Christophe Morisset and Leonid Georgiev

Instituto de Astronomía,
Universidad Nacional Autónoma de México
Apdo. postal 70–264; Ciudad Universitaria
México D.F. 04510; México.
Morisset@astroscu.unam.mx Georgiev@astroscu.unam.mx

Summary. We present results of a combined model for the Planetary Nebula IC418. We perform a coherent model for the star and the nebula, using the codes CMFGEN [4] and Cloudy_3D [2, 7] respectively. We successfully reproduce all the observables (stellar continuum and lines, nebular emission lines, diagnostic line ratios, absolute $H\beta$ flux, HST images). We determine the stellar and nebular characteristics. The presence of an eventual clumping factor avoid to determine more than lower limits for the distance and stellar luminosity.

Key words: Planetary nebula, atmosphere model, photoionization model, IC418

1 Introduction

IC 418 is a well studied young planetary nebula. Its rather simple morphology and the impressive amount of observational data make from this PN an ideal test-case for a deep and detailed modeling performance, associating atmosphere and nebular uptodate modeling tools. We use observations (surface brightness maps, stellar and nebular emission line intensities, UV stellar continuum) from the literature, see below for the details. More details about this work will be found in [8].

2 The star

2.1 Stellar observations

The spectrum of the central star is made from several sources. The wavelengths from 900 to 1100 Å are taken from FUSE spectrum. A STIS/HST spectrum covers the range from 1190 to 1700 Å and finally an IUE SWP spectrum extends the UV spectrum to 1900 Å. In addition to the UV spectrum we obtain a high resolution (R=20000) spectrum of the central star at National Astronomical Observatory in San Pedro Martir (Mexico) using the REOSC echelle spectrograph.

2.2 Atmosphere model

The model is performed using the CMFGEN code [4]. The stellar parameters are set fitting several features of the spectrum described in Sec.2.1. As usual, the terminal velocity is set by the blue wings of [C IV] 1548,50Å and [P IV] 1117,21Å lines.

The turbulent velocity are measured from the width of several photospheric absorption lines visible in the FUSE spectrum. Once the velocity law is established and the temperature is fixed by fitting the nebular response to the ionizing flux, the mass loss rate and the He/H ratio is determined from the fit of the H β and He II 4686Å lines. More details are to be found in [8].

3 The nebula

3.1 Nebular observations

The HST observation are described in [10], [12] and [11]. The Lick observatory observations have been report by [5]. The CTIO observations are taken from [3]. PN IC 418 have been observed in the UV by the IUE observatory and in the IR by the ISO facilities. We take the values for the line intensities corrected from the extinction published by [9].

The optical observations have been obtained through apertures described by [11, 5]. In the following, we will apply the same aperture sizes, orientations and positions to the emission line intensity maps for the optical lines, while the full object is taken into account for the UV and IR intensities. This is done using the facilities of Cloudy_3D.

A total of more than 130 emission lines are used for the model, most of them being pure prediction (not used for the convergence process).

3.2 Nebular model

The model is done using the code Cloudy_3D [2, 7]. The morphology of IC418 was obtained by a trial and error process, using the HST images of H β , [O III] 5007Å and [N II] 6584Å and the density diagnostics (11 line ratios).

The main goal in the determination of this somewhat complex density distribution is to reproduce the central enhanced emission observed in the [O III] 5007Å image. This is reached by using a double ellipsoidal shell morphology, where the density is adjust to reproduce the emission line diagnostics. The density distribution is described in details in [8]. The distance is set to reproduce the observed angular size of the nebula.

To compare the models with the observations we define tolerances according to the observed intensities errors $\frac{\Delta I}{I}$ ranging from 10 to 50%, depending on the absolute intensities. Notice that these errors are also aimed to take into account cross calibration uncertainties between the various observations, and the numerical and modeling errors due to the limited complexity of the morphology we adopt and the errors in atomic data we used. The tolerance is defined as $t = \text{Log}(1 + \frac{\Delta I}{I})$. A Quality Fit parameter is then defined as $QF = \text{Log}(\text{Model}/\text{Observation})/t$. This parameter is also used to analyse the diagnostic line ratios.

4 Results

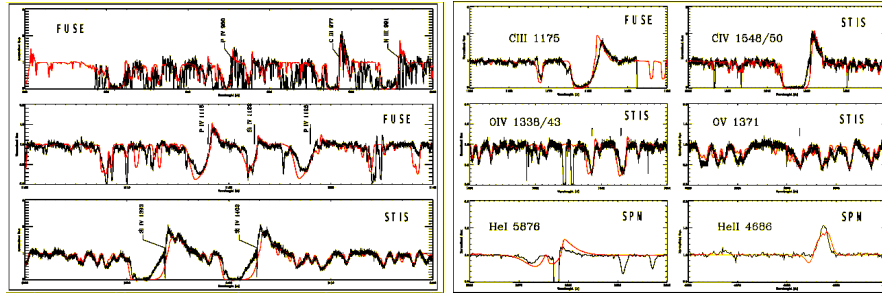


Fig. 1. Comparison between the CMFGEN model and the observations.

Fig. 1 shows the fit to the observed stellar spectrum. An exceptional fit to both the stellar and nebular observations is obtained. Figs. 2, 3 and 4 show comparisons between the nebular observations and the results of the models, in terms of images, line intensities and diagnostic line ratios. Most of the observed intensities are reproduced within the adopted tolerance. The nebular response to the ionizing flux doesn't show any trend when compared to the observations (see Fig.3). This is a clear validation of the combined stellar-nebular model.

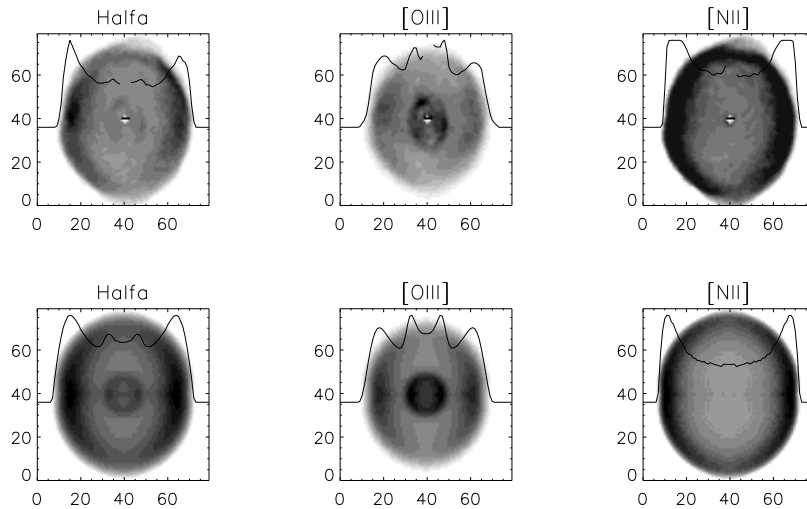


Fig. 2. Comparison between HST observations (upper) and model images (lower). The lines are horizontal cuts in the surface brightness image through the small axis.

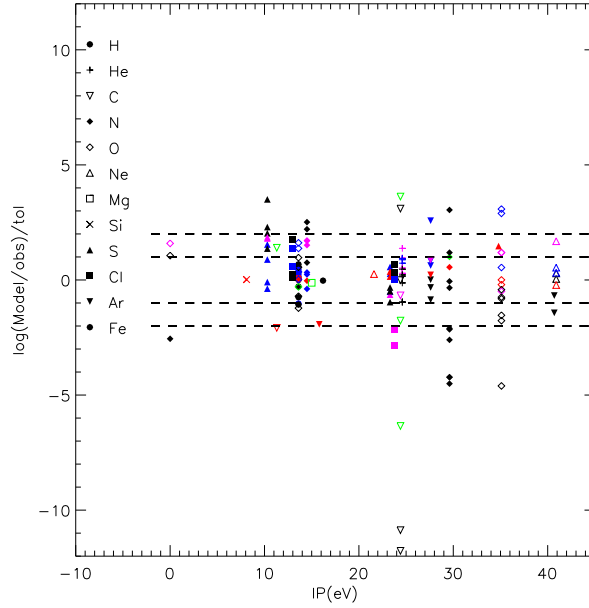


Fig. 3. Results of the model: Quality Fit parameter (defined in Sec.3.2) vs. the ionization potential of the emitting ion.

The clumping factor cf is aimed to take into account an eventual small scale structure of the nebula, where the gas would be concentrated in clumps. We insist on the fact that there is virtually no difference on observables between a model with Q_0 , R and cf and a model with $K^2 \times Q_0$, $K \times R$ and cf/K , where Q_0 is the number of ionizing photons emitted by the central source, R is the radius of the nebula, and K being a coefficient greater than 1. All the line intensities, the angular sizes, and the images are exactly the same for both models. Once the existence of such a clumping factor is accepted, there is no way to determine the distance to the nebula, nor the absolute luminosity of the star, contrary to what is claimed by [6].

In the following, the literature values for the determined parameters are given in parenthesis. The $H\beta$ value (without reddening) is predicted to be 3.4×10^{-10} erg.cm $^{-2}$.s $^{-1}$ (2.6 - 5.9). The distance is estimated to be $K \times 1.0$ kpc (0.3 - 5.7). The ionized hydrogen mass is $K^2 \times 0.03$ solar mass. With an equatorial radius of $K \times 10^{17}$ cm and considering an expansion velocity of 12 km/s, the age of the nebula is $K \times 2750$ years. The effective temperature of the star is 38.5 kK. Its luminosity is $K^2 \times 2300$ solar luminosities (300 - 8000) and the corresponding number of ionizing photons is $K^2 \times 10^{47}$ s $^{-1}$. To reproduce the observed UV continuum flux and shape, an extinction of $E_{B-V} = 0.24$ (0.14 - 0.37) and $R_V = 5.1$ is used with the Cardelli law [1]. The chemical composition of both the star and the nebula we obtain are out of the scope of this proceeding, please refer to [8].

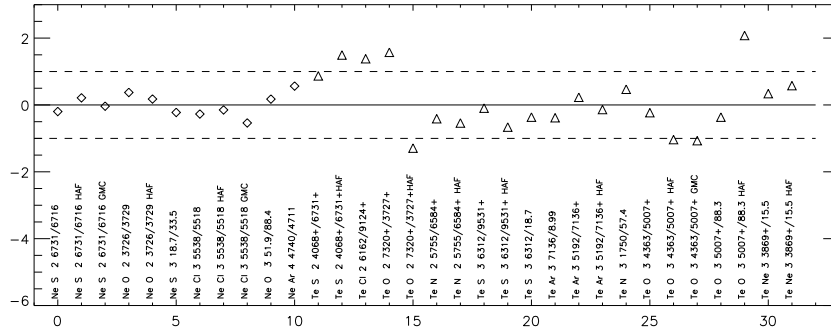


Fig. 4. Quality Fit parameter (defined in Sec.3.2) for various diagnostic ratios (diamonds for electron density and triangles for electron temperature). For the optical lines, HAL refers to [5], GMC to [3], otherwise to [10]. Other observation sources are described in Sec.3.1.

References

1. Cardelli, J. A., Clayton, G. C. and Mathis, J. S. : ApJ, **345**, 245 (1989)
2. Ferland et al.: PASP, **110**, 761 (1998)
3. Gutierrez-Moreno A., Cortes G., Moreno H. : PASP, **97**, 397 (1985)
4. Hillier, D. J. and Miller, D. L.: ApJ, **496**, 407 (1998)
5. Hyung S., Aller L. H., Feibelman W. A. : PASP, **106**, 745 (1994)
6. Monteiro H., Schwarz H. E., Gruenwald R., Guenther K., Heathcote S. R. : ApJ, **620**, 321 (2005)
7. Morisset, C. : Proceedings of IAU symp. 234, M.J. Barlow and R.H. Méndez eds, Cambridge Univ. Press, p.467 (2006)
8. Morisset, C. and Georgiev, L.: in preparation (2009)
9. Pottasch S. R., Bernard-Salas J., Beintema D. A., Feibelman W. A. : A&A, **423**, 593 (2004)
10. Sharpee B., Williams R., Baldwin J. A., van Hoof P. A. M. : ApJS, **149**, 157 (2003)
11. Sharpee B., Baldwin J. A., Williams R. : ApJ, **615**, 323 (2004)
12. Williams R., Jenkins E. B., Baldwin J. A., Sharpee B : PASP, **115**, 178 (2003)